

Capacity design of boundary elements of beam-connected buckling restrained steel plate shear wall

Wen-Yang Liu^{*1}, Guo-Qiang Li^{2a} and Jian Jiang^{3b}

¹ College of Engineering, Heilongjiang Bayi Agricultural University, Daqing, China

² State Key Laboratory of Disaster Reduction in Civil Engineering, Tongji University, Shanghai, China

³ Engineering Laboratory, National Institute of Standards and Technology, Gaithersburg, USA

(Received April 15, 2018, Revised August 21, 2018, Accepted September 14, 2018)

Abstract. As a lateral load resisting component, buckling restrained steel plate shear walls (BRW) have excellent energy dissipating capacity. Similar to thin steel plate shear walls, the mechanical behavior of BRWs depends on the boundary elements (adjacent beams and columns) which need adequate strength and stiffness to ensure the complete yielding of BRWs and the emergence of expected plastic collapse mechanism of frame. This paper presents a theoretical approach to estimate the design forces for boundary elements of beam-connected BRW (i.e., The BRW is only connected to beams at its top and bottom, without connections to columns) using a fundamental plastic collapse mechanism of frame, a force transferring model of beam-connected BRW and linear beam and column analysis. Furthermore, the design method of boundary beams and columns is presented. The proposed approach does not involve nonlinear analyses, which can be easily and efficiently used to estimate the design forces of beams and columns in a frame with BRWs. The predicted design forces of boundary elements are compared with those from nonlinear finite element analyses, and a good agreement is achieved.

Keywords: buckling restrained steel plate shear wall; beam-connected BRW; design forces; boundary elements; plastic collapse mechanism

1. Introduction

Buckling restrained steel plate shear walls (BRW) are one type of lateral load resisting components with excellent energy dissipating capacity. Different from thin steel plate shear walls, BRWs consist of restraining panels fixed on both sides of the infill steel plate by bolts (Fig. 1). The restraining panels are not connected to the beams and columns, thus providing only buckling restraint to the infill steel plate without contribution to the strength and stiffness of framing beams and columns.

The BRW with four-side connections (i.e., the four edges of the steel plate are connected to the surrounding columns and beams) has good mechanical behavior such as high strength and stiffness, and good material efficiency. This is because that the whole steel plate is almost in uniform pure shear condition under lateral load. As an alternative, BRW with two-side connections (only connect to beams at the top and bottom edges) has received more and more attention (Liu *et al.* 2017). This is beneficial for convenient erection of BRWs, flexible arrangement of steel plates and flexible opening for windows and doors.

It is well known that the mechanical behavior of steel plate shear walls depends on the boundary elements

(surrounding beams and columns) which should have adequate strength and stiffness to ensure the yielding of infill steel plates. Even though the design forces for boundary elements of BRWs can be obtained from nonlinear finite element analyses, it is important to propose a simplified analytical method with high efficiency and reasonable accuracy to quickly estimate the design forces of boundary elements, especially in the preliminary design phase.

For thin steel plate shear walls, there is a large amount of research on estimating design forces and capacity design of boundary elements. Park *et al.* (2007) analyzed the tension-field force of steel plate shear walls applied to boundary columns, and presented member design considerations. Berman and Bruneau (2008) proposed a

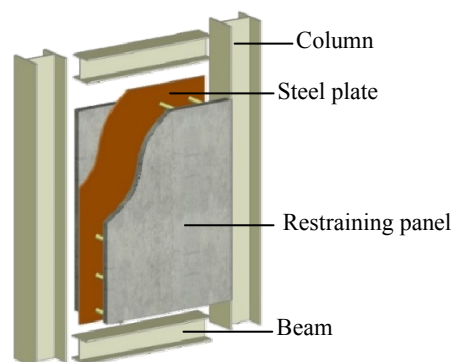


Fig. 1 Configuration of BRW

*Corresponding author, Ph.D., Lecturer,
E-mail: wylu81@126.com

^a Professor

^b Ph.D.

procedure that used fundamental plastic collapse mechanism and linear beam analysis to approximate the design actions for vertical boundary elements of steel plate shear walls (SPSW) for given web plates and horizontal boundary member sizes. The proposed procedure had reasonable accuracy for short SPSWs, and was recommended in AISC seismic provisions (AISC 2010). For mid-rise to high-rise SPSWs, Bhowmick *et al.* (2011) proposed a method to determine the column design forces using linear boundary column models and indirect capacity design principles. The infill plates were designed to yield during design-level earthquakes, resulting in a more economical solution of SPSWs.

Based on the approach proposed by Berman and Bruneau (2008) and AISC seismic provisions (AISC 2010), Jalali and Banazadeh (2016) presented a computer-based approach to determine the force demand exerted on the vertical boundary elements of steel plate shear walls. A programming architecture was proposed to support the implementation of the design algorithm through interaction with ETABS program. Qu and Bruneau (2008, 2010) presented an analytical model for estimating the design forces of intermediate horizontal boundary elements (HBE) of steel plate shear wall systems with reduced beam sections and moment connections. The model combined the assumed plastic mechanism with a linear beam model of intermediate HBEs by assuming fully yielded infill panels. The proposed model was also applied in the steel plate shear wall systems with simple beam-to-column connections to calculate reliable capacity design force demands on the beams and beam-to-column connections (Moghimi and Driver 2014a), and performance-based capacity design for limited-ductility and moderately ductile SPSWs in low and moderate seismic regions (Moghimi and Driver 2014b, c). Qu and Bruneau (2008, 2011) and Qin *et al.* (2017a, b) theoretically investigated the flexural behavior of HBEs of steel plate shear walls. They proposed a procedure to predict the plastic flexural capacity of anchor HBEs of steel plate shear walls, taking into account the boundary effect to reflect the actual stress state at the connection.

As an alternative to four-side connected steel plate shear walls, research has been conducted on estimating design forces for boundary elements of beam-connected steel plate shear walls, i.e., B-SPSW (Thorburn *et al.* 1983, Vatansever and Yardimci 2011, Shekastehband *et al.* 2017) and self-centering beam-connected steel plate shear walls (Clayton *et al.* 2015). In B-SPSW, the steel plate wall is only connected to the adjacent beams at its top and bottom. Ozcelik and Clayton (2018a) provided the equations for calculating axial forces, shear forces, and moment demands of boundary beams of B-SPSWs. To assess the seismic performance of B-SPSWs, a total of 18 B-SPSWs with different geometric characteristics were designed based on the provided equations, and were analyzed under ground motions using the strip model proposed by Ozcelik and Clayton (2017). Ozcelik and Clayton (2018b) investigated the behavior and stability of columns of B-SPSWs, and a parametric study was undertaken to propose a simplified column design method using column axial load demands

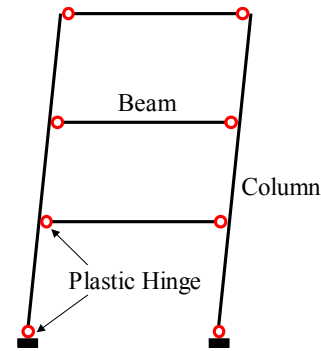


Fig. 2 Schematic of expected plastic mechanism of frames

obtained from Equivalent Lateral Force method (ELF) and accounts for the column buckling strength reduction due to the flexural demands resulting from column rotations at floor levels that are not considered in traditional design approaches.

However, there is little research on the capacity design for boundary elements of beam-connected BRWs. It is important to ensure the complete yielding of BRWs and the occurrence of expected plastic collapse mechanism of frames by carefully designing boundary elements of BRWs. Thus, based on the approaches for determining the design forces for boundary elements of thin steel plate shear walls, this paper presents a theoretical approach to estimate the design forces for boundary elements of beam-connected BRWs using fundamental plastic collapse mechanism of frames (Fig. 2), force transferring model of beam-connected BRWs (Liu 2016) and linear beam/column analysis considering fully yielded BRWs. Since the forces of beams and columns induced by gravity load can be easily added to the results of the proposed method under lateral loads, the gravity load is not taken into account in this study. No nonlinear analyses are involved in the proposed method, making it easy and efficient to estimate the design forces of beams and columns in the frame with BRWs.

2. Forces on frame with BRWs

Liu (2016) proposed a force transferring model of beam-connected BRWs based on the equivalent cross brace model presented by Li *et al.* (2015), as shown in Fig. 3(a). For BRWs with a small height-to-width ratio ($h/b < 1.5$), the equivalent bracing point is $e_0 = 0.1h$ far from the left or right edge of the steel plate. While for BRWs with a large height-to-width ratio ($h/b \geq 1.5$), the equivalent bracing point is $e_0 = b/6$. The area of cross-section and the material strength of braces were determined according to equivalent lateral stiffness and load-bearing capacity to the BRW (Li *et al.* 2015).

Thus, the forces from BRW to boundary beams can be replaced by bracing forces. Fig. 3(b) shows the forces on the i th storey of the frame with BRWs where the lateral loads are applied on both sides of the frame with the same lateral displacement because of rigid floor slab. The parameter V_{ywi} is the lateral load capacity of BRW; V_{fi} is the shear force in the i th storey of frame; $F_i = V_{wi} + V_{fi}$ is the

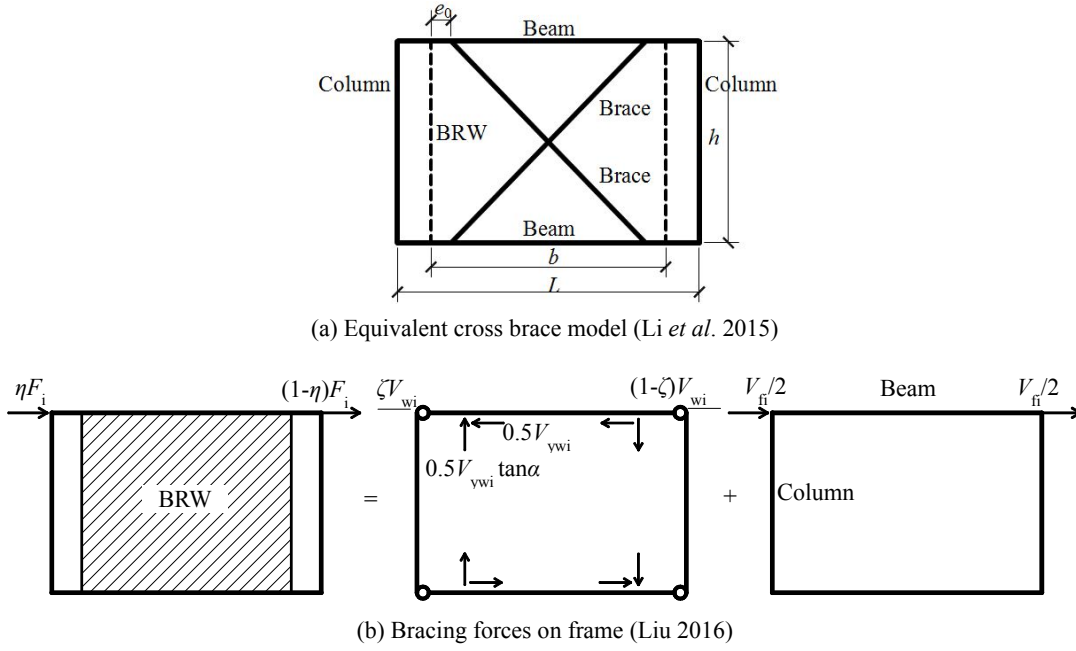


Fig. 3. Equivalent cross brace model and bracing forces on frame

distributed lateral force imposed on the frame with BRWs, which is transferred from the i th floor; η is the coefficient of load transfer from the floor to the frame; ζ is the coefficient of load transfer from BRW to frame; α is the angle between brace and horizontal direction. There is a vertical component ($0.5V_{ywi}\tan\alpha$) and a horizontal component ($0.5V_{ywi}$) of bracing forces at the equivalent bracing point, respectively. In the case of plastic collapse of frames and complete yielding of BRWs, there are plastic hinges at the ends of all beams. Therefore, the frame with BRWs under the lateral load F_i can be decomposed to a hinged frame under the lateral load V_{wi} and bracing forces, and a rigid frame with plastic hinges corresponding to the plastic moment (M_{pbli} and M_{pbri}) at the ends of all beams under the lateral load V_{fi} . Actually, the plastic moment of beams is the superimposition of moment-frame action induced moments and BRW induced moments. Although the sub problems decomposed in the proposed model is different from the actual state, the ultimate moment diagram is the same.

The lateral load capacity of beam-connected BRWs was calculated using Eq. (1) presented by Liu (2016).

For BRW with a small height-to-width ratio, i.e., $h/b < 1.5$

$$V_{yw} = (0.58b - 0.16h)tf_{yw} \quad (1a)$$

For BRW with a large height-to-width ratio, i.e., $h/b \geq 1.5$

$$V_y = 0.51 \frac{b^2}{h} tf_{yw} \quad (1b)$$

where b , h and t is the width, height and thickness of the steel plate in BRWs, respectively; f_{yw} is the yield strength of steel plate.

3. Design forces of boundary beams

3.1 Axial force

As shown in Fig. 4, the axial force is induced by the horizontal components of bracing forces acting on beams. It can be obtained by the equilibrium equation of horizontal forces, which should consider the lateral displacement compatibility under seismic load because of rigid floor slab, i.e., the axial forces of the beam at left and right sides are proportional to e_2 and e_1 . The axial force of the beam at left side can be expressed as

$$N_{bli} = (V_{ywi} - V_{ywi+1}) \frac{e_2}{e_1 + e_2} \quad (2a)$$

The axial force of the beam at right side can be expressed as

$$N_{bri} = (V_{ywi} - V_{ywi+1}) \frac{e_1}{e_1 + e_2} \quad (2b)$$

where N_{bli} and N_{bri} is the axial force at the left and right

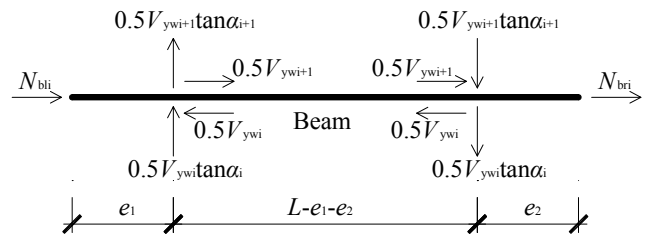


Fig. 4 The axial force and bracing forces on beam

ends of beam in the i th storey, respectively; e_1 is the distance between the left equivalent bracing point and the left beam end; e_2 is the distance between the right equivalent bracing point and the right beam end; V_{ywi} and V_{ywi+1} is the lateral load capacity of BRW in the i th and $i+1$ th storey, respectively.

3.2 Shear force

The shear force in the beam is induced by moment frame sway and the vertical components of bracing forces from BRWs. As shown in Fig. 5, the shear force induced by the vertical components of bracing forces from BRWs in the i th and $i+1$ th storey can be obtained by moment equilibrium equation as

$$V_{bwi} = \frac{0.5V_{ywi} \tan\alpha_i + 0.5V_{ywi+1} \tan\alpha_{i+1}}{L} \times (L - e_1 - e_2) = \frac{V_{ywi}H_i + V_{ywi+1}H_{i+1}}{2L} \quad (3)$$

where $\tan\alpha_i = H_i/(L - e_1 - e_2)$; V_{bwi} is the shear force at the ends of beam in the i th storey induced by BRWs; L is the net span of beams; H_i and H_{i+1} is the i th and $i+1$ th storey height, respectively.

The shear force induced by moment frame sway can be expressed as

$$V_{bfi} = \frac{M_{pbli} + M_{pbri}}{L} \quad (4)$$

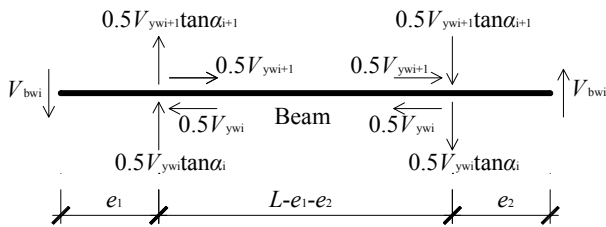


Fig. 5 The shear force and bracing forces on beam

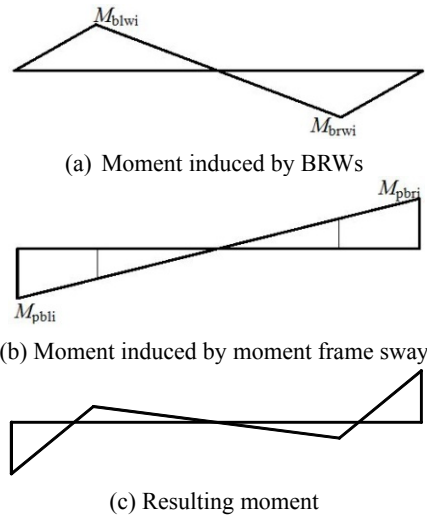


Fig. 6 Decomposition of moment in beam

where V_{bfi} is the shear force at the ends of beam in the i th storey induced by moment frame sway; M_{pbli} and M_{pbri} is the plastic moment at the left and right ends of beam in the i th storey, which should take into account the axial force if the axial force is large especially in the top and bottom beams.

Combining the shear forces in Eqs. (3) and (4) yields the total shear force at the end of beam as

$$V_{bi} = \frac{2M_{pbli} + 2M_{pbri} + V_{ywi}H_i + V_{ywi+1}H_{i+1}}{2L} \quad (5)$$

3.3 Moment

The moment of beams also comes from two sources: BRWs and moment frame sway. As shown in Figs. 5 and 6(a), the moment induced by the vertical components of bracing forces from BRW in the i th and $i+1$ th storey equals to the product of shear force V_{bwi} times the distance between the bracing point and the end of beam, which can be expressed as

$$M_{blwi} = V_{bwi}e_1 = \frac{V_{ywi}H_i + V_{ywi+1}H_{i+1}}{2L}e_1 \quad (6a)$$

$$M_{brwi} = V_{bwi}e_2 = \frac{V_{ywi}H_i + V_{ywi+1}H_{i+1}}{2L}e_2 \quad (6b)$$

where M_{blwi} and M_{brwi} is the moment at left and right bracing point of hinged beam in the i th storey, respectively, induced by BRWs.

For the moment induced by moment frame sway (Fig. 6(b)), axial forces should be taken into account to calculate the plastic moment if the axial force is large especially in the top and bottom beams.

Combining the moment in Figs. 6(a) and (b), the resulting moment is shown in Fig. 6(c).

4. Design forces of boundary columns

4.1 Axial force

As shown in Fig. 7, the axial force of the column in the i th storey can be calculated by summing the shear forces at

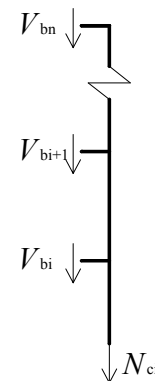


Fig. 7 Vertical forces from beams to column

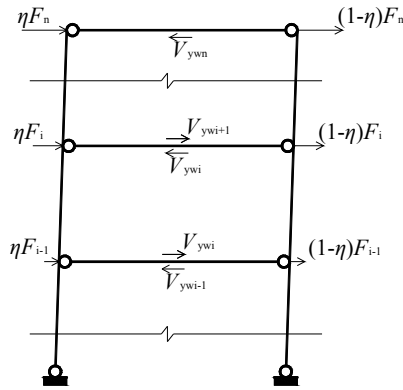


Fig. 8 Plastic collapse mechanism and the lateral load pattern of frame

the end of beams above the column in the i th storey, which can be expressed as

$$N_{ci} = \sum_{j=i}^n V_{bj} \quad (7)$$

4.2 Shear force

In order to calculate the shear force of columns, the capacity of the frame with BRWs should be calculated firstly based on the plastic collapse mechanism of frame, fully yielded BRWs and the lateral load pattern (Fig. 8).

The equilibrium equation is expressed as

$$\begin{aligned} & \sum_{i=1}^n [(F_i - V_{ywi} + V_{ywi+1}) \sum_{j=1}^i H_j] \\ & = \sum_{i=1}^n M_{pbli} + \sum_{i=1}^n M_{pbri} + 2M_{pc1} \end{aligned} \quad (8)$$

where M_{pc1} is the plastic moment at the base of column, which should take into account the axial force. For the top story, V_{ywi+1} should be taken as zero.

Then the shear force of column on the i th storey can be calculated as

$$V_{ci} = (\sum_{j=i}^n F_j - V_{ywi}) / 2 \quad (9)$$

4.3 Moment

The moment of columns can be calculated from the base of column (M_{pc1}) to the top of column (M_{pcn}) according to the shear force of column and the moment equilibrium at beam-to-column joints on each storey.

As shown in Fig. 9, the moment at the top of columns in i th storey can be expressed as

$$M_{cti} = M_{cbi} + V_{ci} H_i \quad (10)$$

where M_{cti} and M_{cbi} is the moment at the top and bottom of column in i th storey, respectively.

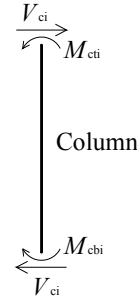


Fig. 9 Internal forces of column

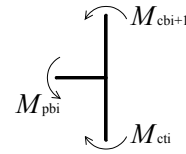


Fig. 10 Moments at beam-to-column joint

As shown in Fig. 10, the moment equilibrium should be kept at the beam-to-column joint, so the moment at the bottom of column in $i+1$ th storey can be expressed as

$$M_{cbi+1} = M_{cti} - M_{pbi} \quad (11)$$

It should be noted that the moment at the base of columns is the plastic moment which should take into account the axial force.

$$M_{cb1} = -M_{pc1} \quad (12)$$

where the positive value of M_c is tension in the right fiber of column, so “-” means the tension is in the left fiber (i.e., the lateral loads act from left to right on the structure).

To keep the moment equilibrium at the beam-to-column joint, the moment at the top of columns in the n th storey is

$$M_{ctn} = M_{pbn} \quad (13)$$

where M_{pbn} should take into account the axial force.

5. Verification against finite element analysis

To check the accuracy of the analytical models proposed in this paper for estimating the design forces for boundary beams and columns of beam-connected BRWs, finite element analyses of three specimens of frames with BRWs with three storey and one span were conducted. In all the three specimens, the section of beams and columns is H500×200×12×16 and H600×300×16×20, respectively. The lateral load capacity of BRWs are $V_{yw1} = 1839$ kN, $V_{yw2} = 1379$ kN and $V_{yw3} = 920$ kN in the first storey, second storey and third storey, respectively. Different thickness, width, yield strength and location of BRWs were used to conduct a parametric study.

The analysis was conducted in finite element software

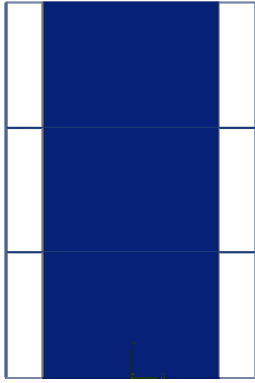
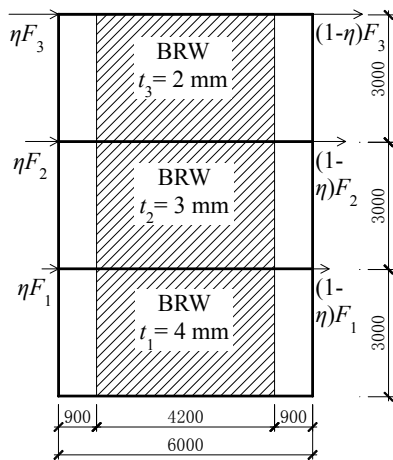
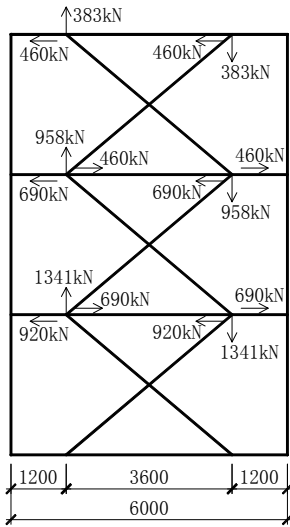


Fig. 11 Finite element model of frame with BRWs



(a) Frame with BRWs



(b) Bracing forces

Fig. 12 Specimen BRW-1

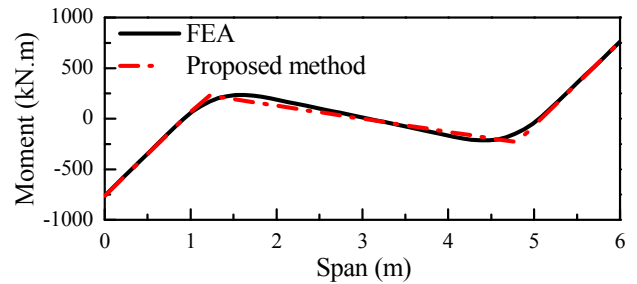
ABAQUS. The B31 and S4R elements were used for framing components and steel plate, respectively. The restraining panels on both sides of the steel plate were simulated by restraining its out-of-plane degree of freedom. Because of the restraining panels, the buckling of the steel plate was completely avoided. The steel plate will yield but

not buckle. Therefore, the initial imperfection was not introduced in FE analyses. Fig. 11 shows the finite element model of the specimen BRW-1. The validation of the finite element model against experimental data has been conducted by Liu *et al.* (2017, 2018). The pushover analysis was conducted on the frame with BRWs under lateral inverted triangular load (i.e., $F_2 = 2F_1$, $F_3 = 3F_1$) controlled by lateral displacement until full yielding of the BRWs and emergence of expected plastic mechanism of frames (Fig. 2). The lateral load was solved theoretically as $F_1 = 470$ kN, $F_2 = 940$ kN, $F_3 = 1410$ kN using Eq. (8). The proposed analysis method in this paper was used to estimate the design forces of boundary beams and columns based on the force transferring model.

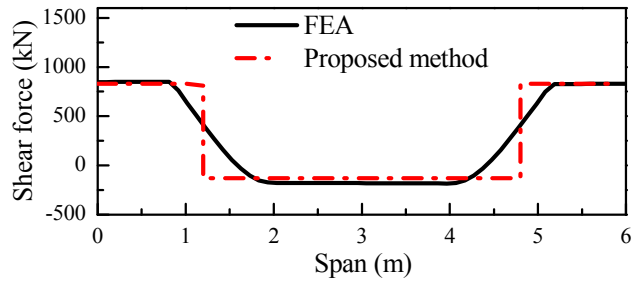
5.1 Specimen BRW-1

The specimen BRW-1 is shown in Fig. 12(a). Fig. 12(b) is the equivalent structure and bracing forces on the frame using the model proposed by Liu (2016).

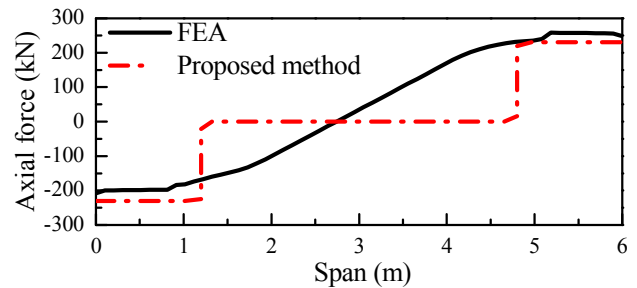
In the first to third storey, the thickness of the steel plate is 4 mm, 3 mm and 2 mm corresponding to the lateral load capacity of $V_{yw1} = 1839$ kN, $V_{yw2} = 1379$ kN and $V_{yw3} = 920$



(a) Moment of beam in the second storey

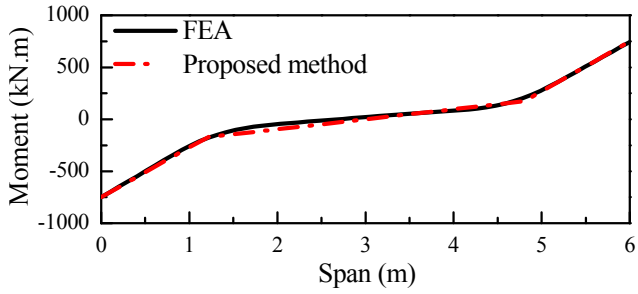


(b) Shear force of beam in the second storey

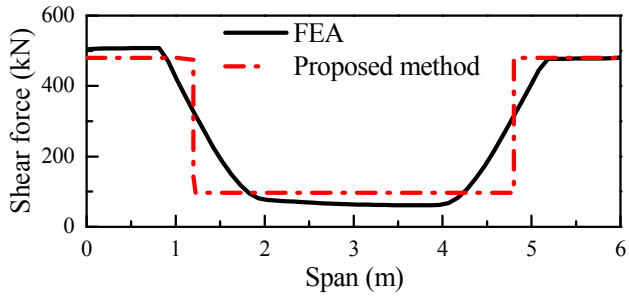


(c) Axial force of beam in the second storey

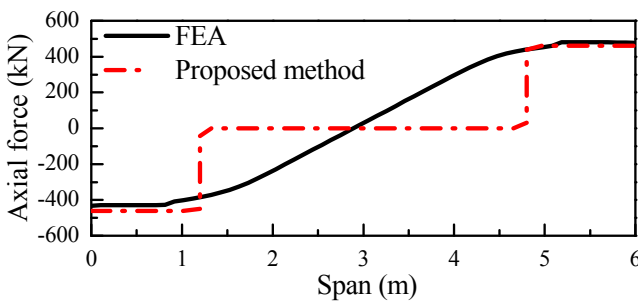
Fig. 13 Force diagrams for boundary beams and columns in specimen BRW-1



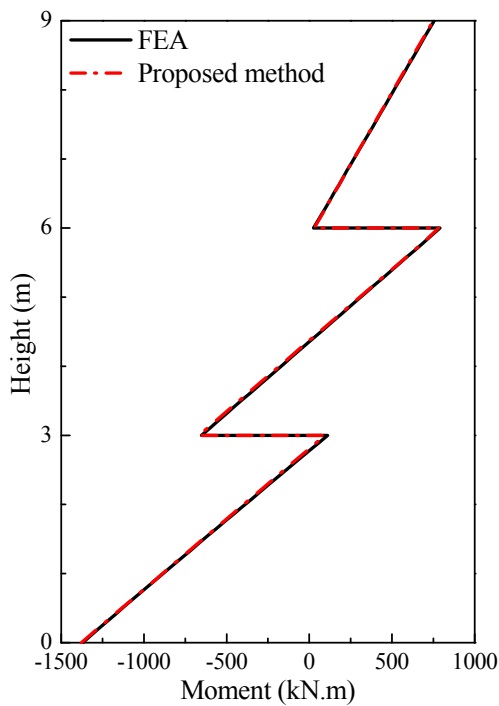
(d) Moment of beam in the third storey



(e) Shear force of beam in the third storey



(f) Axial force of beam in the third storey

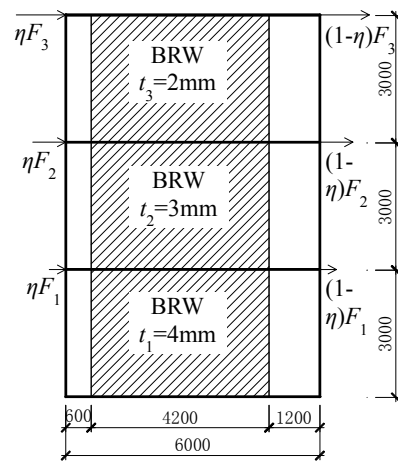


(g) Moment of right column

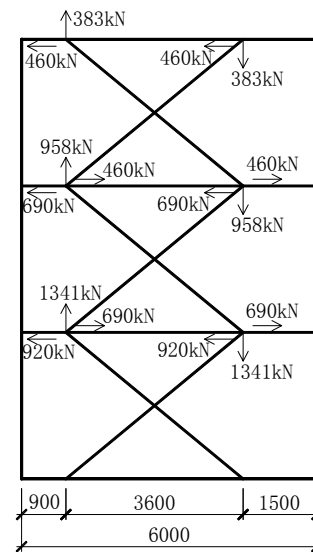
Fig. 13 Continued

Table 1 Axial forces of beams and columns in specimen BRW-1

Elements	Storey	Axial force		
		FEA (kN)	Proposed method (kN)	Error (%)
Beams (left end)	3	-433	-460	6.2
	2	-208	-230	10.6
	1	-219	-230	5.0
Beams (right end)	3	477	460	-3.6
	2	248	230	-7.3
	1	233	230	-1.3
Columns (left side)	3	514	480	-6.6
	2	1369	1309	-4.4
	1	2416	2368	-2.0
Columns (right side)	3	-471	-480	1.9
	2	-1293	-1309	1.2
	1	-2342	-2368	1.1



(a) Frame with BRWs



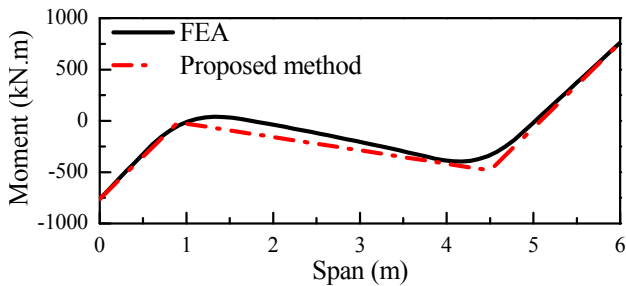
(b) Bracing forces

Fig. 14 Specimen BRW-2

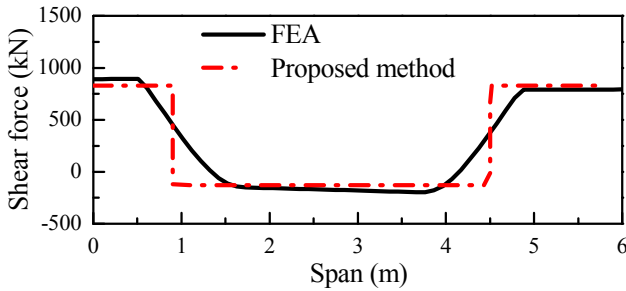
kN, respectively. This is to ensure the complete yielding of BRWs. The yield strength of the frame and steel plate is $f_y = 345$ MPa and $f_{yw} = 235$ MPa, respectively, with perfectly elasto-plastic behavior. Fig. 13 and Table 1 show the comparison of design forces of beams and columns in the specimen BRW-1, which were predicted using FE analysis and the proposed procedure in this paper.

5.2 Specimen BRW-2

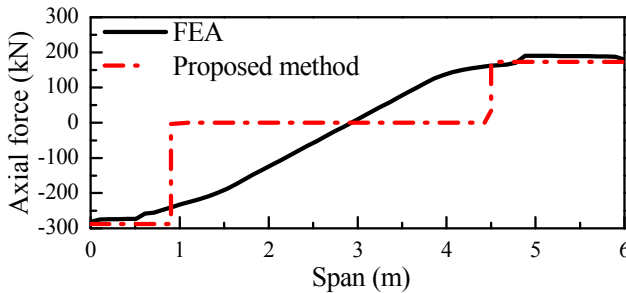
The specimen BRW-2 is shown in Fig. 14(a). Fig. 14(b) is the equivalent structure and bracing forces on the frame.



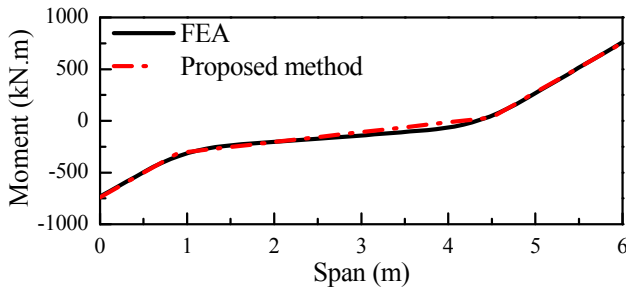
(a) Moment of beam in the second storey



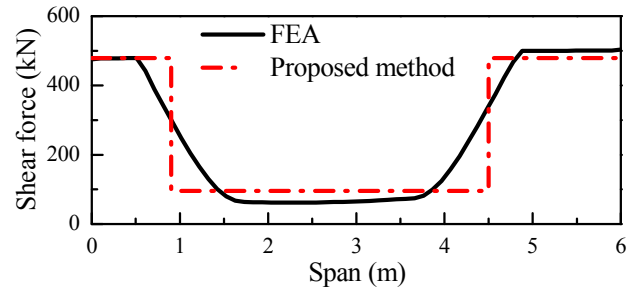
(b) Shear force of beam in the second storey



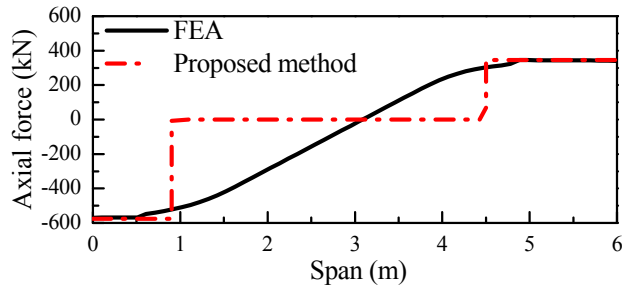
(c) Axial force of beam in the second storey



(d) Moment of beam in the third storey



(e) Shear force of beam in the third storey



(f) Axial force of beam in the third storey

Fig. 15 Continued

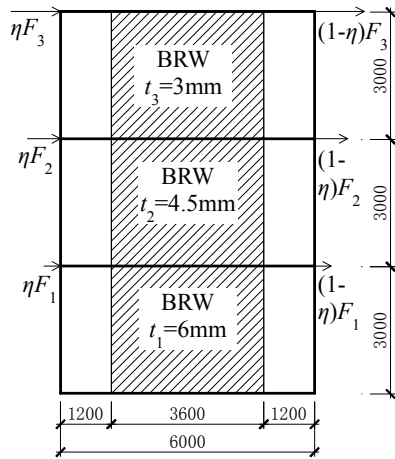
The only difference between the specimen BRW-1 and specimen BRW-2 is the location of BRWs. The BRWs were arranged at the midspan of the beam for the specimen BRW-1, while the BRWs were arranged asymmetrically in BRW-2 with different distances to the ends of the beam.

Fig. 15 and Table 2 show the comparison of design forces of beams and columns in specimen BRW-2 estimated using FE analysis and the proposed procedure. The moment of columns in the specimen BRW-2 was the same as that in the specimen BRW-1 shown in Fig. 13(g).

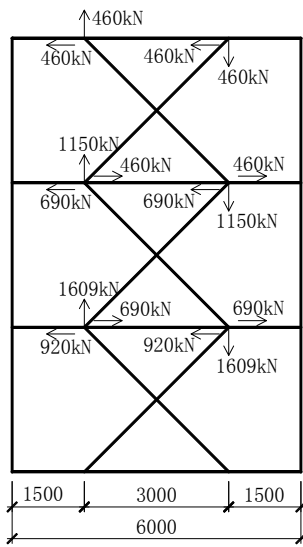
Table 2 Axial forces of beams and columns in specimen BRW-2

Elements	Storey	Axial force		
		FEA (kN)	Proposed method (kN)	Error (%)
Beams (left end)	3	-571	-575	0.7
	2	-281	-288	2.5
	1	-275	-288	4.7
Beams (right end)	3	339	345	1.8
	2	179	173	-3.4
	1	182	173	-4.9
Columns (left side)	3	487	479	-1.6
	2	1388	1308	-5.8
	1	2538	2367	-6.7
Columns (right side)	3	-495	-479	-3.2
	2	-1280	-1308	2.2
	1	-2246	-2367	5.4

Fig. 15 Force diagrams for boundary beams in specimen BRW-2



(a) Frame with BRWs



(b) Bracing forces

Fig. 16 Specimen BRW-3

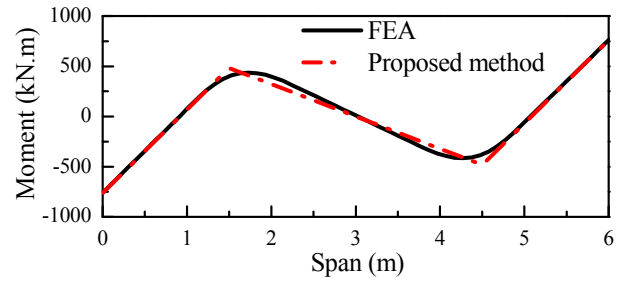
5.3 Specimen BRW-3

Figs. 16(a) and (b) show the layout of the specimen BRW-3, and equivalent structure with bracing forces, respectively. The difference between specimen BRW-3 and specimen BRW-1 is the size and yield strength of BRWs. The width of BRW is 3.6 m for BRW-3, compared to 4.2 m for BRW-1. In order to achieve the same yield capacity of BRW as that in specimen BRW-1, the yield strength of BRW for BRW-3 was assumed to be $f_{yw} = 190.6$ MPa, and the thickness of BRWs were set to be 6 mm, 4.5 mm and 3 mm in the first, second and third storey, respectively.

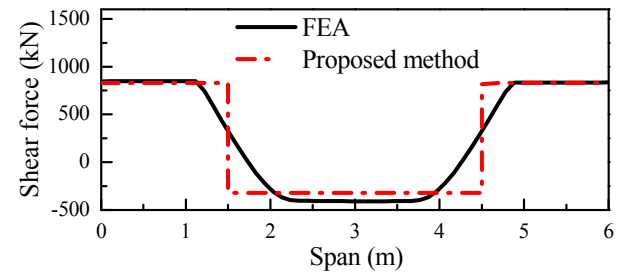
A comparison of predicted design forces of beams and columns in specimen BRW-3 between FE analysis and the proposed procedure is shown in Fig. 17 and Table 3. The moment of columns in specimen BRW-3 was also the same as that in specimen BRW-1 shown in Fig. 13(g).

The above three examples show a good agreement of design forces of boundary elements between the proposed analytical approach and FE analysis for different sizes and locations of BRWs. Therefore, the proposed analytical model can be used to estimate the design forces of beams

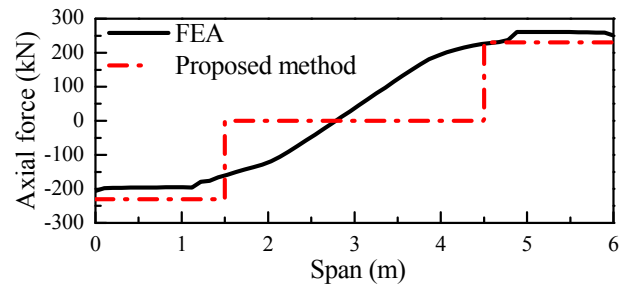
and columns in the frame with BRWs with high efficiency, especially in preliminary design phase.



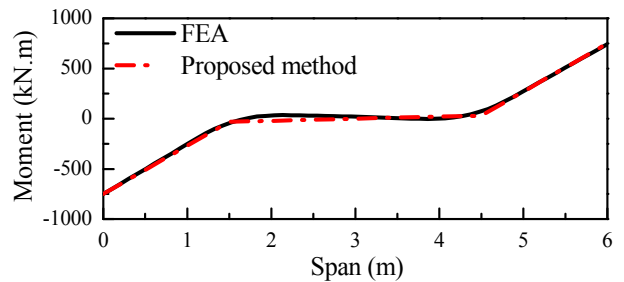
(a) Moment of beam in the second storey



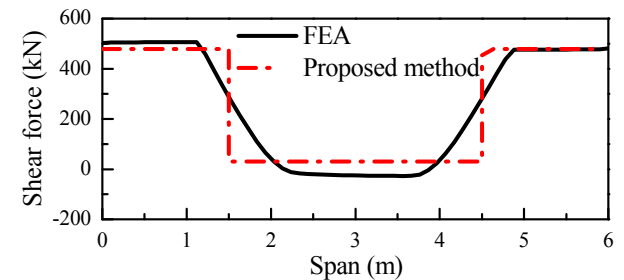
(b) Shear force of beam in the second storey



(c) Axial force of beam in the second storey

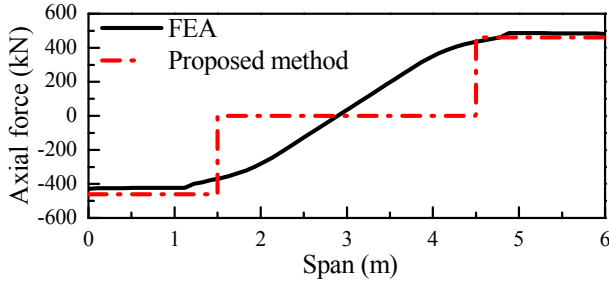


(d) Moment of beam in the third storey



(e) Shear force of beam in the third storey

Fig. 17 Force diagrams for boundary beams in specimen BRW-3



(f) Axial force of beam in the third storey

Fig. 17 Continued

Table 3 Axial forces of beams and columns in specimen BRW-3

Elements	Storey	Axial force		
		FEA (kN)	Proposed method (kN)	Error (%)
Beams (left end)	3	-428	-460	7.5
	2	-206	-230	11.7
	1	-217	-230	6.0
Beams (right end)	3	481	460	-4.4
	2	251	230	-8.4
	1	236	230	-2.5
Columns (left side)	3	512	480	-6.3
	2	1368	1309	-4.3
	1	2415	2368	-1.9
Columns (right side)	3	-470	-480	2.1
	2	-1296	-1309	1.0
	1	-2345	-2368	1.0

For the specimen BRW-1 (Table 1) and BRW-3 (Table 3), the absolute values of axial forces of beams at the left end are almost as same as those at the right end. This is because the BRWs are arranged at the midspan, and the length of the left beam segment is equal to the right one. For the specimen BRW-2 (Table 2), the BRWs are not arranged at the midspan, so the absolute values of axial forces of beams at the left end are much greater than that at right end. Therefore, Eq. (2) based on the assumption of lateral displacement compatibility under seismic load because of rigid floor slab was verified.

The three examples also show that for BRWs with the same lateral load capacity the beam moment induced by wide BRWs (Figs. 13(a), (d)) is less than that induced by narrow BRWs (Figs. 17(a), (d)). The beam moment induced by BRWs arranged at midspan (Figs. 13(a), (d)) is less than that induced by BRWs arranged deviating from midspan (Figs. 15(a), (d)). It indicates that for a given capacity demand of BRW, an increment in the width of steel plate will decrease the capacity demand of boundary beams, and it is preferred to arrange BRWs at midspan.

6. Preliminary design suggestions for boundary elements

6.1 Preliminary design suggestions for boundary beams

Eq. (5) indicates that the size and location of BRWs have little influence on the shear force in boundary beams if the capacity demand of BRWs is determined. This is also verified by FE analyses as shown in Figs. 13, 15 and 17. However, the location of equivalent bracing points may affect the axial forces and moments in boundary beams as shown in Eqs. (2) and (6), which means that the size and location of BRWs have significant influence on the axial forces and moments in boundary beams. As shown in Fig. 6(a) and Eq. (6), with the increase of the distance between the equivalent bracing point and the beam end, the moment in beam will increase.

For the design of boundary beams of BRWs, the following procedure is proposed in this paper. Firstly, the shear capacity V_{bcri} should be greater than the actual shear force calculated using Eq. (5), i.e.

$$V_{bcri} > V_{bi} \quad (14)$$

Then, in order to achieve the expected plastic mechanism of frame, there should be no plastic hinge in beams except the ends, as shown in Fig. 2. Thus the moment at equivalent bracing point of beam as shown in Fig. 6(c) should not be greater than the elastic ultimate moment assuming to be $0.9 \times 0.9 \times M_{pbi} = 0.8M_{pbi}$ for a H section. In this equation, the first coefficient 0.9 is the ratio of elastic section modulus to plastic section modulus, and the second coefficient 0.9 is the ratio of design strength to yield strength of boundary element material, i.e.

$$M_{bwi} - \frac{L/2 - e}{L/2} M_{pbi} \leq 0.8M_{pbi} \quad (15)$$

The plastic moment demand of boundary beam can be solved from Eq. (15) as

$$M_{pbi} \geq \frac{L}{1.8L - 2e} M_{bwi} = \frac{(V_{ywi}H_i + V_{ywi+1}H_{i+1})e}{3.6L - 4e} \quad (16)$$

Furthermore, for strengthening the existing structure, the section of beams cannot be changed, the design of beam can be achieved by changing the width of BRWs. Based on Eq. (15), the distance between the equivalent bracing point and the beam end can be expressed as

$$e \leq \frac{3.6LM_{pbi}}{V_{ywi}H_i + V_{ywi+1}H_{i+1} + 4M_{pbi}} \quad (17)$$

For a given capacity demand of BRWs, the width and location of BRWs should meet the requirement in Eq. (17) to avoid the formation of plastic hinges at equivalent bracing points. For BRWs with a small height-to-width ratio ($h/b < 1.5$), it means

$$b \geq L - 2e + 0.2h \quad (18a)$$

While for BRWs with a large height-to-width ratio ($h/b \geq 1.5$), it means

$$b \geq \frac{3}{2}(L - 2e) \quad (18b)$$

Furthermore, the best location of BRWs is at midspan of the beam.

For the given capacity of BRWs and the cross-section area of beams in the above three specimens, the distance between the equivalent bracing point and the beam end should be less than 1.29 m, 1.65 m and 2.81 m in the first, second and third storey, respectively. Thus, there may be internal plastic hinges along the span of beams in the first storey for the specimen BRW-2 and BRW-3. In contrast, the design of the specimen BRW-1 is acceptable.

6.2 Preliminary design suggestions for boundary columns

In order to achieve the expected plastic mechanism of frames, there should be no plastic hinge in columns except the base as shown in Fig. 2. Therefore, at any section of the column except the base, the moment and axial force should meet the requirement in Eq. (18) as

$$\frac{M_{ci}}{W_{ci}} + \frac{N_{ci}}{A_{ci}} \leq f \quad (19)$$

It means that the moment of columns should not be greater than the elastic ultimate moment taking into account the axial force, i.e.

$$M_{ci} \leq \left(f - \frac{N_{ci}}{A_{ci}}\right) \times W_{ci} \quad (20)$$

where f is the design strength of boundary element material; A_{ci} and W_{ci} is the section area and elastic section modulus of columns, respectively.

For given equivalent bracing forces from BRWs and internal forces of boundary beams, the design of boundary columns can be accomplished by meeting the requirement in Eq. (20) through an iterative process. Furthermore, the section of columns should also meet the principle of strong columns and weak beams.

Using the proposed design method, the minimum elastic section modulus demand of columns in the above three specimens is 3151 cm³, and the actual elastic section modulus is 4146 cm³. To be more economical, the column section in the three specimens can be changed to H600×300×12×18. The corresponding elastic section modulus is 3648 cm³ which is greater than the minimum elastic section modulus demand (3590 cm³) determined using Eq. (20).

7. Conclusions

This paper presented an analytical approach to predict the design forces of boundary elements of beam-connected

BRWs. By using the equivalent brace model, the forces transferred from BRWs to the frame can be replaced by bracing forces, and the design forces of beams and columns can be obtained by linear analyses. The proposed approach, based on a fundamental plastic collapse mechanism of frame and linear beam and column analysis, provided an easy and efficient way to estimate the design forces of boundary beams and columns, especially in preliminary design phase. Furthermore, the proposed method was verified against FE analyses, and a good agreement was achieved. It indicates that the proposed method can be used for the design of boundary elements of BRWs to ensure the complete yielding of BRWs and the emergence of expected plastic collapse mechanism (plastic hinges at the ends of beams and column base).

The proposed method and FE analyses indicate that for a given capacity demand of BRWs, wider steel plates will lead to lower capacity demand of boundary beams. It is recommended to arrange BRWs at midspan of beams.

It should be mentioned that the gravity load is not taken into account in this research, because the forces of beams and columns induced by gravity loads can be easily added to the results of the proposed procedure under lateral loads. Furthermore, the equations presented in this paper are valid when the location of bracing points is the same along beam for all BRWs (i.e., e_1 and e_2 are the same for all stories). If the location of bracing points is different (e.g., different width or different height of BRWs), the equations of design forces for boundary elements of BRWs can be also obtained by the same procedure.

Acknowledgments

This research was supported by National Natural Science Foundation of China (Grant No. 51608180), Natural Science Foundation of Heilongjiang Province (Grant No. QC2016071), Program for Young Scholars with Creative Talents in Heilongjiang Bayi Agricultural University (Grant No. CXRC2016-05, 2016-KYYWF-0165) and Doctoral research fund of Heilongjiang Bayi Agricultural University (Grant No. XDB-2017-05).

References

- AISC, ANSI/AISC 341-10 (2010), Seismic provisions for structural steel buildings, American Institute of Steel Construction; Chicago, IL, USA.
- Berman, J.W. and Bruneau, M. (2008), "Capacity design of vertical boundary elements in steel plate shear walls", *Eng. J.*, **45**(1), 57-71.
- Bhowmick, A.K., Driver, R.G. and Grondin, G.Y. (2011), "Application of indirect capacity design principles for seismic design of steel-plate shear walls", *J. Struct. Eng.*, **137**(4), 521-530.
- Clayton, P.M., Berman, J.W. and Lowes, L.N. (2015), "Seismic performance of self-centering steel plate shear walls with beam-only-connected web plates", *J. Constr. Steel Res.*, **106**, 198-208.
- Jalali, S.A. and Banazadeh, M. (2016), "Computer-based evaluation of design methods used for a steel plate shear wall system", *Struct. Des. Tall Special Build.*, **25**(17), 904-925.

- Li, G.Q., Liu, W.Y., Lu, Y. and Sun, F.F. (2015), "Stressing mechanism and equivalent brace model for buckling restrained steel plate shear wall with two-sided connections", *J. Build. Struct.*, **36**(4), 33-41. [In Chinese]
- Liu, W.Y. (2016), "Study on mechanical performance of reinforced concrete frame with buckling restrained steel plate shear wall", Ph.D. Dissertation; Tongji University, Shanghai, China.
- Liu, W.Y., Li, G.Q. and Jiang, J. (2017), "Mechanical behavior of buckling restrained steel plate shear walls with two-side connections", *Eng. Struct.*, **138**, 283-292.
- Liu, W.Y., Li, G.Q. and Jiang, J. (2018), "Experimental study on reinforced concrete frames with two-side connected buckling-restrained steel plate shear walls", *Adv. Struct. Eng.*, **21**(3), 460-473.
- Moghimi, H. and Driver, R.G. (2014a), "Beam design force demands in steel plate shear walls with simple boundary frame connections", *J. Struct. Eng.*, **140**(7), 04014046.
- Moghimi, H. and Driver, R.G. (2014b), "Performance-based capacity design of steel plate shear walls. I: development principles", *Journal of Structural Engineering*, **140**(12), 04014097.
- Moghimi, H. and Driver, R.G. (2014c), "Performance-based capacity design of steel plate shear walls. II: design provisions", *J. Struct. Eng.*, **140**(12), 04014098.
- Ozcelik, Y. and Clayton, P.M. (2017), "Strip model for steel plate shear walls with beam-connected web plates", *Eng. Struct.*, **136**, 369-379.
- Ozcelik, Y. and Clayton, P.M. (2018a), "Seismic design and performance of SPSWs with beam-connected web plates", *J. Constr. Steel Res.*, **142**, 55-67.
- Ozcelik, Y. and Clayton, P.M. (2018b), "Behavior of columns of steel plate shear walls with beam-connected web plates", *Eng. Struct.*, **172**, 820-832.
- Park, H.G., Kwack, J.H. and Jeon, S.W. (2007), "Framed steel plate wall behavior under cyclic lateral loading", *J. Struct. Eng.*, **133**(3), 378-388.
- Qin, Y., Lu, J.Y., Huang, L.C.X. and Cao, S. (2017a), "Flexural behavior of beams in steel plate shear walls", *Steel Compos. Struct., Int. J.*, **23**(4), 473-481.
- Qin, Y., Lu, J.Y., Huang, L.C.X. and Cao, S. (2017b), "Flexural behavior of anchor horizontal boundary element in steel plate shear wall", *Int. J. Steel Struct.*, **17**(3), 1073-1086.
- Qu, B. and Bruneau, M. (2008), "Seismic behavior and design of boundary frame members of steel plate shear walls", Technical Rep. No. MCEER-08-0012, Multidisciplinary Center for Earthquake Engineering Research, Buffalo, New York, NY, USA.
- Qu, B. and Bruneau, M. (2010), "Capacity design of intermediate horizontal boundary elements of steel plate shear walls", *J. Struct. Eng.*, **136**(6), 665-675.
- Qu, B. and Bruneau, M. (2011), "Plastic moment of intermediate horizontal boundary elements of steel plate shear walls", *Eng. J., AISC*, **48**(1), 49-64.
- Shekastehband, B., Azaraxsh, A.A. and Showkati, H. (2017), "Hysteretic behavior of perforated steel plate shear walls with beam-only connected infill plates", *Steel Compos. Struct., Int. J.*, **25**(4), 505-521.
- Thorburn C.J., Kulak L.J. and Montgomery G.L. (1983), "Analysis of steel plate shear walls", Structural Engineering Report No. 107, University of Alberta, Edmonton, Alberta, Canada.
- Vatansever, C. and Yardimci, N. (2011), "Experimental investigation of thin steel plate shear walls with different infill-to-boundary frame connections", *Steel Compos. Struct., Int. J.*, **11**(3), 251-271.